foods

MDPI

Article

Multi-Omics and Chemometric Analysis of Aroma and Shelf Life Dynamics in Raisin Syrup Sourdough and Commercial Yeast Breads

Junhan Zhang [1], Tatsuro Maeda [2,*], Seiya Nakamura [3], Kenjiro Sugiyama [3], Yoko Iijima [3], Takayoshi Tanaka [1], Shuntaro Isoya [2], Kazuya Hasegawa [2] and Tetsuya Araki [1]

[1] Graduate School of Agriculture and Life Sciences, University of Tokyo, Tokyo 113-003, Japan; zhang-junhan@g.ecc.u-tokyo.ac.jp (J.Z.); t-takayoshi@g.ecc.u-tokyo.ac.jp (T.T.); aaraki@g.ecc.u-tokyo.ac.jp (T.A.)
[2] Department of Health and Dietetics, Teikyo Heisei University, Tokyo 170-8445, Japan; s.isoya0705@gmail.com (S.I.); k.hasegawa@thu.ac.jp (K.H.)
[3] Department of Applied Chemistry, School of Advanced Engineering, Kogakuin University, Tokyo 192-0015, Japan; s220063@g.kogakuin.jp (S.N.); bt13171@ns.kogakuin.ac.jp (K.S.); st13686@ns.kogakuin.ac.jp (Y.I.)
* Correspondence: t.maeda@thu.ac.jp

Abstract

Raisin syrup sourdough is a popular traditional leavening method in Japan, yet its specific impact on bread aroma evolution and shelf life stability remains scientifically underexplored. This study characterized the fermentation dynamics and volatile profiles of raisin syrup sourdough bread compared to a commercial yeast control over a 3-day shelf life, utilizing comprehensive two-dimensional gas chromatography–mass spectrometry (GC × GC-TOFMS) and primary metabolite profiling of sugars, amino acids, and organic acids. The analysis resolved over 760 volatiles and revealed a fundamental kinetic divergence. While the yeast control exhibited a 24 h metabolic lag, the raisin sourdough achieved rapid activation, establishing a higher initial volatile load immediately post-baking. Driven by lactic acid bacteria dominance and extensive proteolysis, the sourdough's acidic environment facilitated the retention of fruity esters and malty branched-chain aldehydes while effectively suppressing lipid oxidation markers like 9,17-Octadecadienal. Key aromatic markers, including benzenepropanol and Octanoate <isopentyl->, were significantly elevated and stabilized in the sourdough group. These findings demonstrate that raisin syrup fermentation generates a superior, stable aromatic profile, providing a scientific basis for optimizing clean-label artisan bread production in the Japanese market.

Keywords: GC × GC-TOFMS; bread aroma; shelf life; sourdough; volatile organic compounds; functional group profiling; chemometric analysis

Check for updates

Academic Editors: María José Cardador, Pablo Rodríguez-Hernández and Lourdes Arce

Received: 10 January 2026
Revised: 7 February 2026
Accepted: 12 February 2026
Published: 15 February 2026

Copyright: © 2026 by the authors. Licensee MDPI, Basel, Switzerland. This article is an open access article distributed under the terms and conditions of the Creative Commons Attribution (CC BY) license.

1. Introduction

Sourdough fermentation is a multifunctional bioprocess that enhances the sensory, nutritional, and shelf life attributes of bread. By utilizing a stable symbiosis of lactic acid bacteria (LAB) and yeasts, sourdough improves dough rheology and flavor complexity compared to conventional yeast fermentation [1]. These benefits stem from metabolic activities that produce organic acids, exopolysaccharides, and a wide array of volatile organic compounds (VOCs). Consistent with the sourdough fermentation literature, this has led to sourdough being framed as a clean-label and sustainable alternative to chemical

improvers, given its use of naturally occurring microbiota and locally maintainable starters that can lower reliance on additives and associated environmental impacts [1,2].

In Japan, the bread market, which is traditionally dominated by commercial yeast-based Shokupan (white pan bread), is shifting. Evolving consumer preferences for diverse, naturally derived flavor profiles are driving interest in artisanal products [3] prompting bakeries to explore sourdough for novel aroma characteristics. In this regard, Shokupan represents a highly standardized, mild-flavored bread matrix in which subtle fermentation- and storage-derived aroma shifts can be sensitively detected, quantified, and mechanistically interpreted. Moreover, Japan-specific processing conditions and ingredients create a unique biochemical environment. This allows for an evaluation of how local factors influence volatile formation and aroma stability, moving beyond the findings of conventional sourdough studies. This changing landscape has been driving locally adapted practices, most notably raisin syrup sourdough. This method involves the spontaneous fermentation of raisins in syrup to cultivate a consortium of indigenous wild yeasts and LAB from raisin skins [4]. Despite its growing popularity, industrial uptake is constrained because VOC profiling is rarely time-resolved across shelf life and validated markers for shelf life prediction are still lacking, particularly validated VOC markers for shelf life prediction, leaving raisin-derived aroma changes during storage difficult to forecast and manage in practical production and supply chain settings.

While certain aromatic aspects of conventional sourdough have been identified, these studies rely primarily on one-dimensional gas chromatography (1D-GC) and headspace solid-phase microextraction (HS-SPME) which can be constrained from limited peak capacity and co-elution in complex matrices. And few studies have characterized the comprehensive flavor and quality evolution during the shelf life of raisin syrup sourdough-based white bread. This research gap necessitates a high-resolution analytical platform paired with advanced chemometric tools to resolve the overlapping chemical signals associated with storage-induced quality degradation. To address this challenge, comprehensive two-dimensional gas chromatography coupled with time-of-flight MS (GC × GC -TOFMS) offers transformative potential. By employing orthogonal columns and thermal modulation, this system achieves a peak capacity 5–10 times higher than conventional 1D-GC, resolving intricate co-eluting compounds and trace-level analytes [5]. Such enhanced separation generates high-dimensional datasets with substantial detail, enabling objective pattern recognition to highlight key VOCs as candidate markers. Although this approach has revolutionized metabolomics in various biological matrices [6–8], its application potential in assessing the aroma stability and fermentation dynamics of raisin syrup starters remains largely unexplored. Comprehensive and validated VOC markers that can monitor and predict aroma stability across shelf life in raisin syrup sourdough are still lacking.

To address these gaps, this study aims to characterize time resolved VOC dynamics from Day 0 to Day 3 shelf life and to identify a concise set of key volatile markers that explain group differences and support industrially relevant monitoring. To achieve this, comprehensive GC × GC TOFMS was applied as a high-precision platform to overcome coelution in the complex sourdough matrix, while chemometric analyses were used to interpret time course shifts in VOC profiles and prioritize key volatile markers, supported by complementary primary metabolite measurements.

2. Materials and Methods

2.1. Sample Preparation

2.1.1. Preparation of Raisin Syrup Starter

The raisin syrup starter was developed based on a traditional artisanal formulation [9]. Specific ratios and parameters of the ingredients are detailed in Table 1. High-quality

organic raisins were combined with sugar, and malt syrup and warm water (30 °C) was used to aid raisin rehydration and early fermentation [10]. The mixture was stirred thoroughly in a clean container. Fermentation was conducted at 27 °C for a duration of 4 to 5 days, consistent with reported artisanal starter conditions supporting yeast and LAB activity [11]. To ensure consistent fermentation and prevent mold growth on the surface, the mixture was agitated at least once daily. Completion of the starter was identified when all raisins floated to the surface and active bubbling was observed. Upon completion, the solids were filtered out, and the resulting fermented liquid was refrigerated for subsequent use in dough preparation.

Table 1. Formulation of Raisin Syrup Starter.

Ingredient	Ratio (%)
Water (30 °C)	100
Raisins	50
Caster Sugar (Johakuto)	25
Non-diastatic Malt Syrup (2× dilution)	2
Total	177

2.1.2. Dough Preparation and Fermentation

Two types of French-style white bread were prepared to evaluate the impact of different leavening agents on aroma evolution during shelf life, including a control bread leavened with commercial fresh yeast and an experimental bread leavened with raisin syrup sourdough starter. The bread-making process followed the method of TSUMUGI bakery [9]. The specific formulations for both dough types are detailed in Table 2. The specific formulations for both dough types are detailed in Table 2.

Table 2. Formulations for Control (Yeast) and Raisin (Sourdough) Breads.

Ingredients	Control	Sourdough
Wheat Flour (Soledore)	100% (3000 g)	100% (3000 g)
Commercial Yeast	0.5% (15 g)	—
Raisin Sourdough Starter	—	8% (240 g)
Non-diastatic malt syrup (2× dilution)	0.6% (18 g)	0.6% (18 g)
Salt	2% (60 g)	2% (60 g)
Water	70% (2100 g)	63% (1890 g)
Total Weight	173.1% (5193 g)	173.6% (5208 g)

The mixing process followed a standardized regime involving 2 min at low speed followed by 8–9 min at medium speed to achieve a target dough temperature of 25.2–25.9 °C to support gluten development and subsequent fermentation, consistent with standard practice and the bakery protocol [11]. Following mixing, the dough underwent a 60 min floor time, with a degassing punch performed at the 30 min mark. Fermentation was conducted in two distinct stages, where temperature, relative humidity (RH), and duration were identified as critical variables. Controlling these parameters prevented surface dehydration and expansion irregularities, thereby ensuring representative headspace sampling for the metabolic profile analysis. The initial cold fermentation at 2 °C for 4 h was applied to slow fermentation and allow controlled maturation, followed by bulk fermentation at 27 °C and 75% RH for 8 h to provide stable fermentation conditions while minimizing surface drying, consistent with established retarded fermentation practices [9].

2.1.3. Proofing and Baking

After bulk fermentation, the dough was divided into 200 g portions and subjected to a 40 min bench time. The loaves were then shaped using a molder into a baton configuration and proofed on cloth for 70 min at 32 °C and 75% RH. Prior to baking, a saucisson style cut was applied to the surface to maintain crumb uniformity. Baking was conducted at a local artisanal bakery in Tokyo, Japan, using a professional electric deck oven (Soleo Evo, Bongard, Strasbourg, France) for 27 min with an initial temperature of 250 °C (top) and 225 °C (bottom), which was subsequently reduced to 225 °C and 210 °C, respectively. These conditions were applied to standardize loaf structure and baking performance for shelf life VOC analysis, consistent with established protocols [9].

2.1.4. Storage and Sampling

Following baking, loaves were cooled and uniformly sliced into 13 pieces (18 mm per slice). All breads were sealed in polyethylene bags and kept at room temperature (25 °C) with a relative humidity of 50% for subsequent sampling. To ensure spatial representativeness, three slices were systematically selected from the 13 slices (the 3rd, 7th, and 11th slices) for further analysis. Samples were collected at predefined time points (Day 0–Day 3), where Day 0 was defined as within 2 h after cooling. The bread crumb was sampled by excising the center portion of each selected slice and cutting it into 5 mm × 5 mm × 5 mm cubes, followed by homogenization for subsequent volatile analyses, whereas an aliquot of the same crumb material was processed into a uniform freeze-dried powder prior to primary metabolite analysis. Analyses were conducted in triplicate (n = 3) for each treatment at various time points.

2.2. Aroma Capture and Volatile Extraction

Volatile analyses were conducted under identical conditions for all replicates (n = 3, as described above), and repeatability was confirmed using an RSD criterion ($\leq$15%) for relative peak areas. Subsequently, 2 g of the prepared sample was hermetically sealed in 20 mL precision-thread headspace vials equipped with PTFE/silicone septa to maintain an airtight environment. The analysis was performed using a sequential dual-step Dynamic Headspace-Multi Volatile Method (DHS–MVM) implemented on a GERSTEL Multipurpose Sampler (MPS) RoboticPro System (GERSTEL GmbH & Co. KG, Mülheim an der Ruhr, Germany), a methodology specifically suited for the analysis of high-ethanol and high moisture samples [12].

The DHS–MVM approach capture the aroma profile utilizing the distinct affinities of two specialized adsorbents with operation parameters detailed in Table 3. The volatile collection proceeds in a two-stage process. In the first stage, Carbopack BX is employed to trap highly volatile and polar constituents, including low-boiling compounds that represent top-to-middle notes. This stage involves a low-temperature incubation followed by a dedicated drying phase, which effectively removes ethanol and residual moisture to prevent column saturation. Subsequently, Tenax TA is used in the second stage to capture mid-range to high-boiling point volatiles, specifically targeting middle-to-base notes and heavier semi-volatile aroma compounds [13]. By elevating the incubation temperature and increasing the trapping volume, the system facilitates the release and collection of less volatile, higher molecular weight compounds to achieve a more comprehensive aroma capture. Following these sequential collection phases, the volatiles accumulated on both adsorbents were thermally desorbed, concentrated, and injected into the GC system for analysis.

Table 3. Operation parameter of Dynamic Headspace–Multi-Volatile Method for aroma capturing.

Parameter	Step 1: Adsorbent Carbopack BX (Top/Middle)	Step 2: Adsorbent Tenax TA (Middle/Base)
Incubation Temp	25 °C	80 °C
Trapping Volume	650 mL	3500 mL
Trapping Flow	100 mL/min	100 mL/min
Trap Temp	30 °C	40 °C
Drying Volume	300 mL	0 mL
Transfer Heater	150 °C	150 °C

2.3. GC × GC-TOFMS Analysis

Volatile compounds were further analyzed using a LECO Pegasus BT 4D GC × GC–TOFMS (LECO Corporation, St. Joseph, MI, USA). The system utilized an automated injection sequence where desorbed analytes were transferred to the chromatographic interface. The injector temperature was maintained at 230 °C, while the transfer line and ion source temperatures were held at 250 °C and 255 °C, respectively.

Chromatographic separation was achieved using a two-dimensional setup consisting of a polar primary column (InertCap Pure-Wax, GL Sciences Inc., Tokyo, Japan) [14] to facilitate polar separation, followed by a non-polar secondary column (InertCap 5MS, GL Sciences Inc., Tokyo, Japan) [15] for boiling point separation. The primary column oven was programmed to start at 40 °C (held for 1 min), increased to 100 °C at a rate of 10 °C min^{-1}, and finally ramped to 250 °C at 5 °C min^{-1} with a final hold time of 10 min.

A modulation period of 6.5 s was employed to ensure effective trapping and release of analytes between the two dimensions. High-purity helium served as the carrier gas, and the TOF-MS was operated with a mass range of m/z 35–600 and an acquisition rate of 200 spectra/sec. Relative abundances were obtained from total ion chromatograms (TIC) following standard metabolite-profiling practices. A blank extract was used to identify and eliminate system-derived artifacts. Peaks likely associated with column bleeding or instrument-related contaminants were reduced by excluding compounds containing terms such as “glycol”, “silan”, “siloxan” or “crown” from the dataset. In addition, compound names were manually reviewed to remove obvious duplicates or inconsistent entries. These steps were intended to minimize the inclusion of instrumental noise and improve the likelihood that the remaining chromatographic peaks represented meaningful VOC features.

2.4. Chromatographic Identification and Statistical Screening

Data acquisition and processing were conducted using ChromaTOF software (version 5.54.48.070156; LECO Corporation, St. Joseph, MI, USA). Qualitative identification of VOCs was achieved through a combination of external retention-index calibration and spectral-library matching. Specifically, a C9–C40 n-alkane mixture standard (cat. no. 1021-58325, GL Sciences Inc., Tokyo, Japan; 50 μg mL^{-1} each) was analyzed under identical GC × GC-TOF-MS conditions to establish reference 1D and 2D retention times. To maximize the discovery of low-abundance and previously unreported VOCs, thereby establishing a comprehensive baseline for future studies. Mass spectra were matched against the NIST 20 Mass Spectral Library (National Institute of Standards and Technology, Gaithersburg, MD, USA) and Wiley 11 Mass Spectral Library (Wiley, Hoboken, NJ, USA). A similarity threshold of 650 was applied for these matches; consequently, all resulting identifications are considered tentative.

For data normalization, peak areas were calculated as a percentage of the total peak area within each sample. These relative abundance values are reported as the mean ± SD

of three biological replicates, as no absolute quantification was performed. Statistical exploration was subsequently carried out using JMP Pro 17 (SAS Institute Inc., Cary, NC, USA), which included Principal Component Analysis (PCA), Hierarchical Clustering Analysis (HCA), and heatmap visualization. Initial indicators of potential differences between groups were assessed using Student's *t*-test and one-way ANOVA, with a significance threshold set at $p < 0.05$.

To identify differentially expressed VOCs, volcano plot analyses were performed using Rstudio version 4.4.0 (Posit PBC, Boston, MA, USA) through a total of ten pairwise comparisons structured to capture the volatile profile across two distinct analytical dimensions (Table 4). Longitudinal analysis to track temporal changes within each group, and cross-sectional analysis to evaluate disparities in aroma profile at each sampling point. Within this framework, a feature was deemed a potentially differential marker only when it satisfied a dual-threshold criterion of statistical significance at $p < 0.05$ and a fold-change magnitude of $|\log_2(FC)| \geq 1.0$. These thresholds were applied to filter the dataset, ensuring that only compounds with the most biological and chemical relevance were retained for subsequent mechanistic interpretation.

Table 4. Experimental Design for Pairwise Differential Comparisons.

Comparison Dimension	Reference Group (Control)	Target Group (Experimental)	Objective	Count
Longitudinal	Day 0 (Baseline)	Day 1, Day 2, Day 3	To identify aroma profile shifts induced by storage time	6 pairs
Cross-Sectional	Yeast Sourdough	Raisin Sourdough	To identify disparities of aroma profile at each specific time point.	4 pairs

Overall, a hierarchical chemometric workflow was applied to interpret the complex VOC dataset across shelf life. The Heatmap provided a global overview of temporal changes across all identified compounds during storage. PCA reduced data dimensionality to evaluate clustering and verify whether raisin water sourdough and control breads occupied distinct chemical spaces across D0–D3, providing a basis to reflect overall temporal shifts in chemical classes. Volcano plots were then served as a statistical filter to identify the VOCs most responsible for these differences using dual thresholds ($p < 0.05$ and $|\log_2(FC)| \geq 1.0$). Candidate markers were then evaluated across storage time to confirm consistent trends, enabling reliable identification of key aromatic biomarkers associated with raisin water sourdough aroma and its shelf life evolution.

2.5. Marker Tracking and Time-Course Visualization of Aroma Profile

A backward-tracing approach, initiated from candidate volatile markers identified via volcano plot analysis, was employed to monitor the continuous evolution of prioritized candidate markers. This method integrated dumbbell plots with sparkline-normalized trend lines to visualize temporal shifts from the post-baking starting point (Day 0) to the end of shelf life (Day 3). To facilitate a direct comparison between markers across varying concentration magnitudes (e.g., 10^5 vs. 10^8), data were normalized to a unified scale. Day 3 was used as the reference time point for visualization and for comparing endpoint patterns

Volatile markers were initially screened from the previous volcano-plot results based on their $-\log_{10}(p)$ values and effect size ($|\log_2 FC|$) from the volcano plots. To avoid selection bias from fold-change inflation in compounds with near-zero baselines, a stratified selection strategy was implemented. Components were categorized by their direction of change between Day 0 and Day 3 as either depletion-type (Day 3 < Day 0) or generation-type (Day 3 > Day 0). Representative markers from both categories were then retrieved

from the significant regions of the volcano plots to ensure a balanced representation of the aroma transformations. To define a clear relevance hierarchy, key markers were prioritized by integrating volcano-plot–based statistical confidence $-\log_{10}(p)$ and change magnitude ($|\log_2 FC|$) with abundance context at both the shelf life start (Day 0 raw peak area) and endpoint (Day 3 relative abundance), thereby emphasizing markers that are statistically robust and practically relevant in both baseline intensity and endpoint presence.

A manual quality control process was further applied to identify and exclude exogenous contaminants (e.g., plasticizers) via mass spectral library matching. Markers were visualized in two panels based on their relative abundance at Day 3 (criteria defined below). Panels were defined by Day 3 group-wise relative abundance to display the comparison at the end of shelf life alongside time-course patterns.

2.6. Primary Metabolites Analysis

Primary metabolites, including free amino acids, sugars, and organic acids, were analyzed as supportive measurements to aid the interpretation of the volatile profiles. Methanol, chloroform, ribitol, and pyridine were obtained from Wako Pure Chemical Industries, Ltd. (Osaka, Japan). Methoxyamine hydrochloride, 2-isopropylmalic acid, and alkane standard solution were purchased from Merck KGaA (Darmstadt, Germany). N-methyl-N-(trimethylsilyl)trifluoroacetamide (MSTFA) was sourced from GL Science, Inc. (Tokyo, Japan) [12]. Primary metabolite analyses were performed for all replicates (n = 3, as described in Section 2.1.4), and analytical repeatability was assessed using an RSD threshold of <10% to ensure the consistency of the primary metabolite quantification.

2.6.1. Free Amino Acid Profiling via HPLC

Free amino acids were extracted by dissolving 100 mg of the freeze-dried bread powder in 1 mL of 75% ethanol. This mixture underwent 5 min of sonication followed by 30 min of shaking at 4 °C to ensure thorough extraction. Following centrifugation at 16,000× g for 20 min at 4 °C, the resulting supernatant was dried using a centrifugal evaporator (Tokyo Rikakikai Co., Ltd., Tokyo, Japan). The dried residue was subsequently redissolved in 200 µL of 10 mM HCl. For detection, the extract was derivatized using an AccQ-Tag Ultra Derivatization Kit (Waters Corporation, Milford, MA, USA) and analyzed with an Acquity UPLC H-Class amino acid analyzer (Waters Corporation, Milford, MA, USA) according to the manufacturer's protocol.

2.6.2. Sugar and Organic Acid Profiling via GC-MS

Sugars and organic acids were analyzed using a modified gas chromatography–mass spectrometry method as described previously [16]. The process began by dissolving 25 mg of the bread powder in a methanol:water:chloroform (2.5:1:1, $v/v/v$) solution. Ribitol and 2-isopropylmalic acid were introduced as internal standards during this stage. The samples were homogenized for 2 min at 30 Hz using a TissueLyser II (Qiagen, Hilden, Germany) and incubated at 37 °C for 30 min. After centrifugation at 16,000× g for 5 min at 4 °C, 800 µL of the supernatant was partitioned with water and centrifuged again to separate the polar phase. Then, 800 µL aliquot of the supernatant was then transferred to a new tube and partitioned by adding 400 µL of water. After brief mixing and a second centrifugation (16,000× g, 5 min, 4 °C), the resulting polar phase was collected, concentrated in a centrifugal evaporator for approximately 90 min, and subsequently freeze-dried for further analysis.

For derivatization, 50 µL of methoxyamine hydrochloride in pyridine (20 mg/mL) was added to the freeze-dried samples and incubated at 37 °C for 90 min. Subsequently, 50 µL of MSTFA was added, followed by further incubation at 37 °C for 30 min. The resulting derivatized samples were then subjected to GC-MS analysis. GC-MS analysis was

conducted using a GCMS-QP2010 system (Shimadzu Corporation, Kyoto, Japan) equipped with an AOC-20i/s autosampler and a CP-Sil 8 CB column (30 m × 0.25 mm i.d., 0.25 µm film thickness; Agilent Technologies, Inc., Santa Clara, CA, USA). Samples were injected in split mode, utilizing a 100:1 ratio for sugar analysis and a 20:1 ratio for organic acid analysis, with an injection temperature of 230 °C. Helium served as the carrier gas at a constant flow rate of 1.0 mL/min.

The oven temperature program commenced at 80 °C (held for 2 min), increased at a rate of 10 °C/min to a final temperature of 325 °C, and was maintained for an additional 10 min. The interface and ion source temperatures were set to 250 °C and 200 °C, respectively. Ions were generated via electron ionization at 0.93 kV, with data recorded at a scan rate of 20 scans/s over a mass range of m/z 85–500.

Metabolite data were processed in Rstudio version 4.4.0 (Posit PBC, Boston, MA, USA) using the pheatmap package. Heatmaps were generated to visualize row-scaled relative abundances of metabolite group means, employing a navy-white-red color gradient to represent low, mean, and high values, respectively. Statistical significance was determined via one-way ANOVA followed by Tukey's HSD test ($p < 0.05$), with significant differences indicated by letter annotations directly on the heatmap tiles.

2.7. Strain-Based Comparative Analysis

A strain-based comparative strategy was adopted based on limited literature addressing the specific impact of raisin syrup sourdough on white bread aroma and shelf life. Dominant microorganisms commonly reported in raisin syrup/grape fermentations were compiled from the literature as a reference framework to interpret specific sourdough microbial compositions with the observed changes in aroma development and shelf life stability.

3. Results and Discussion

3.1. Heatmap and Cluster Analysis

The total number of detected aroma compounds remained stable across all groups, fluctuating minimally between 760 and 765 throughout the shelf life. Specifically, counts for the Yeast and Raisin groups shifted only slightly from D0 to D3 (764 to 761 and 760 to 764, respectively) (Figure 1). Despite this numerical stability, hierarchical cluster analysis (HCA) indicated pronounced changes in relative abundance over time (Figure 1), reflecting compositional restructuring rather than changes in compound count.

The HCA dendrogram revealed a clear divergence in maturation kinetics between the two groups. The yeast control showed a delayed transition during the first 24 h, remaining close to the baseline state, whereas the Raisin sourdough shifted earlier and aligned with the later-stage profiles. This pattern suggests that raisin-driven fermentation accelerates the initial evolution of aroma volatiles, enabling the raisin group to reach a matured composition more rapidly, consistent with the trend reported in [17]. This rapid shift in the Raisin group highlights its superior efficiency in initiating fermentation and rapidly establishing a mature volatile signature.

These temporal dynamics were visually corroborated by the heatmap, which displayed clearly defined data structures organized into two opposing metabolic blocks, representing a clear transition between the starting materials and the final products An early-stage cluster consisted of compounds with high initial abundance at D0 that were depleted in later stages, likely representing substrate-derived precursors. Conversely, a distinct late-stage cluster—comprising metabolites absent at baseline—became highly abundant by D2 and D3, characterizing the establishment of a mature fermentation metabolome [18]. The stark contrast between these two blocks effectively maps the biochemical progression

of the samples, moving from raw, precursor-rich profiles to complex, fermentation-derived aroma profiles.

These dynamics were also reflected in the heatmap, which organized compounds into two major blocks, showing early-stage cluster with high abundance of VOCs at D0 that decreased over time, and a late-stage cluster that was low or absent at baseline but increased markedly by D2–D3, indicating the emergence of fermentation-derived aroma metabolites [18]. Together, these patterns summarize a transition in samples from precursor-rich profiles to mature, fermentation-derived aroma profiles.

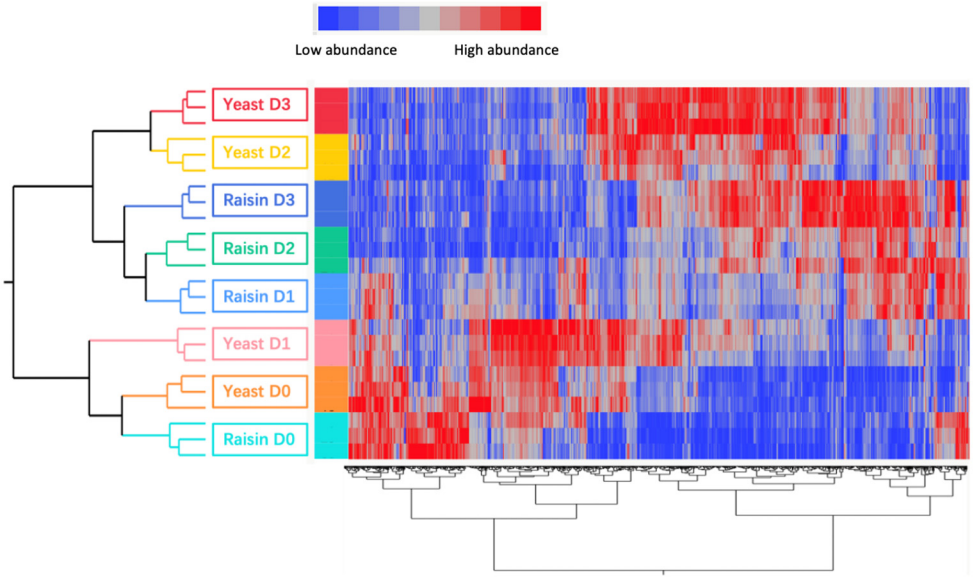

Figure 1. Heatmap and hierarchical clustering analysis of aroma compounds in Yeast and Raisin samples across four time points (D0–D3). The dendrogram on the left illustrates the clustering of sample groups based on similarity in their profiles. The dendrogram at the bottom represents the clustering of individual compounds. The color bar represents Z score standardized abundance for each compound across samples (red, higher than the compound mean; blue, lower than the compound mean). Samples are labeled by group (Yeast/Raisin) and day (D0, D1, D2, D3).

3.2. PCA

Principal Component Analysis (PCA) was employed to visualize metabolic trajectories, with the first two components accounting for 76.96% of the total variance (Figure 2a,b). PC2 clearly delineated the samples by biological origin—Yeast in the positive region and Raisin in the negative—indicating that both groups maintain intrinsically distinct chemical signatures throughout fermentation. This separation suggests that the unique microflora and precursor compounds inherent to raisin water create a volatile profile that remains fundamentally different from industrial yeast, regardless of fermentation time.

PC1 (47.2%) primarily reflected the shared time-dependent evolution of the volatile profile from the baseline state (D0) toward a more mature composition (D2/D3), suggesting that both groups underwent a common set of underlying reactions. However, their kinetics diverged as the yeast control progressed more slowly during the first 24 h, whereas the Raisin sourdough shifted earlier along the same trend. Interestingly, PC3 (9.16%) revealed a non-linear pattern, as evidenced by the arch-shaped distribution where D1 and D2 samples exhibited higher scores. This suggests a temporary increase or peak of specific intermediate volatile compounds during the middle stages of storage. This earlier stabilization, complemented by the transitional fluctuations captured by PC3, indicates an accelerated maturation process in the Raisin bread, reaching a matured volatile profile more rapidly than the industrial yeast control, in agreement with previous observations [19].

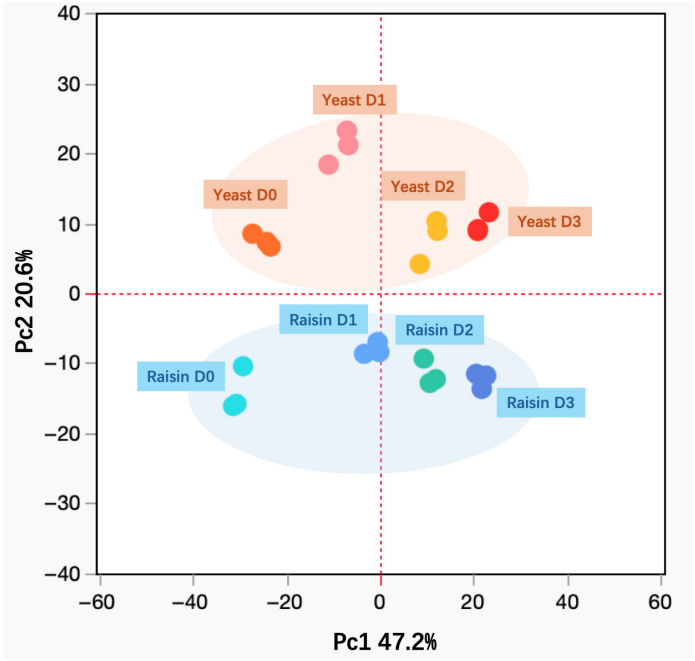

(**a**)

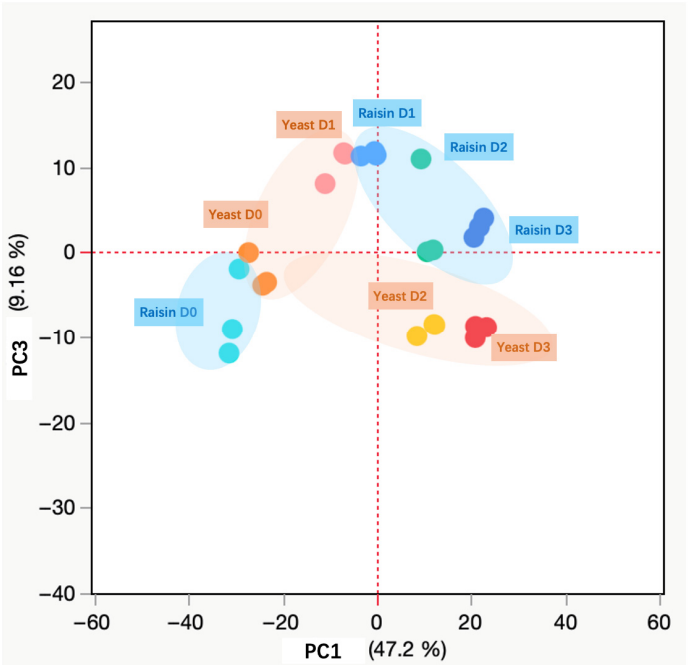

(**b**)

Figure 2. Principal Component Analysis (PCA) score plots of aroma compounds in Yeast and Raisin samples during storage. (**a**) PC1 versus PC2 and (**b**) PC1 versus PC3. The first three principal components collectively account for 76.96% of the total variance, with PC1, PC2, and PC3 explaining 47.2%, 20.6%, and 9.16%, respectively. Samples are colored by group and storage day where Yeast samples are in shades of orange and Raisin samples are in shades of blue.

3.3. Primary Metabolites Analysis and Strain-Based Comparative Analysis

To provide necessary biochemical context for the following evolution of functional groups and candidate aroma markers during shelf life, key primary metabolites were briefly evaluated. This assessment, supplemented by a strain-based comparison with existing literature on dominant sourdough microorganisms, establishes a reference framework for interpreting the mechanisms driving aroma development. By defining substrate availability and the physiochemical environment, these data provide insights into how raisin

sourdough fermentation reshapes the dough matrix, thereby contributing to a mechanistic basis for the aromatic shifts observed during storage.

The Raisin-Sourdough group exhibited a significant enrichment of total free amino acids compared to the Yeast control. This elevation is particularly pronounced in hydrophobic residues such as phenylalanine, leucine, and isoleucine (Figure 3). Beyond indicating active proteolysis, these specific residues serve as critical substrates for the Ehrlich Pathway, fueling the synthesis of complex aroma-active compounds. The abundance of these precursors suggests that the raisin-based system is more biochemically prepared for intensive flavor development than commercial yeast control.

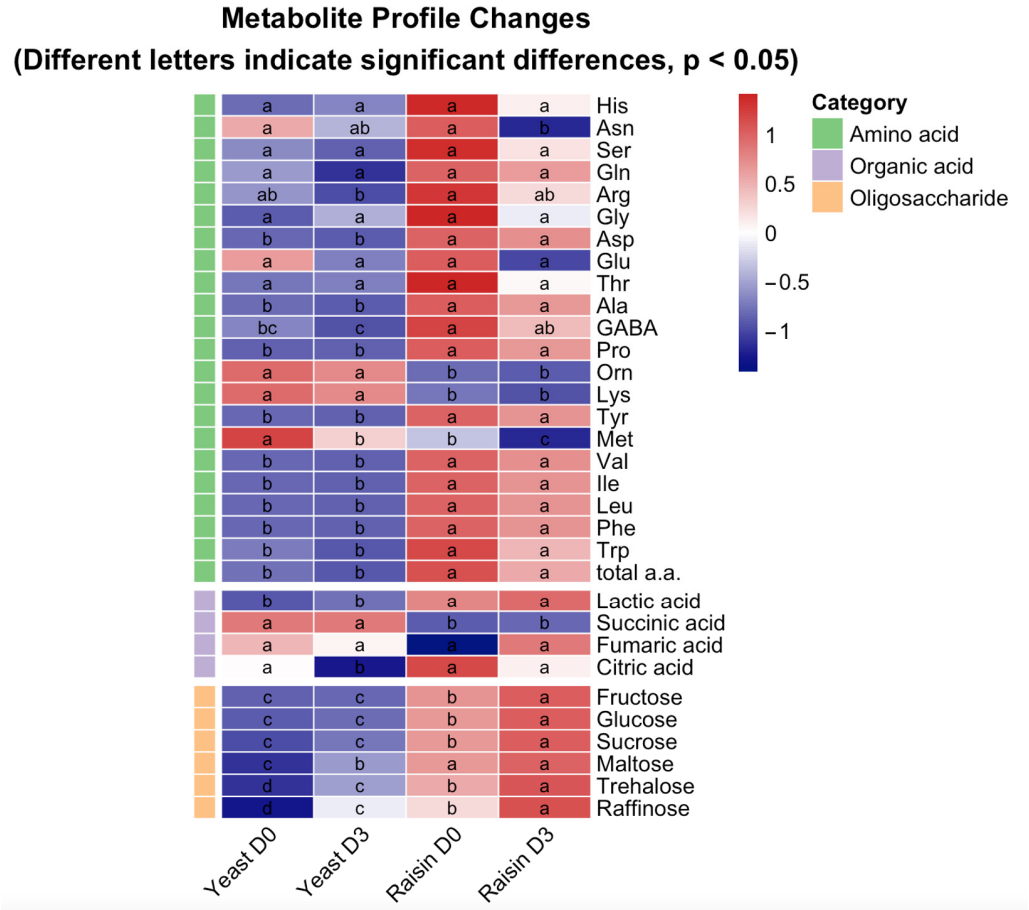

Figure 3. Heatmap visualization of metabolite profiles in Yeast and Raisin groups during shelf life (D0 vs. D3). The color scale represents the relative abundance of each metabolite, normalized by row (Z-score); red indicates higher relative content, and blue indicates lower relative content. The colored bars on the left classify metabolites into Amino acids (green), Organic acids (purple), and Oligosaccharides (orange). Statistical analysis was performed using one-way ANOVA followed by Tukey's HSD post hoc test. Different lowercase letters (a–d) within each row indicate statistically significant differences between groups ($p < 0.05$). Groups sharing the same letter are not significantly different. Data are presented as means ($n = 3$).

In terms of organic acids, the profiles differed markedly. The Raisin group is dominated by lactic and citric acids, whereas the Yeast group exhibits higher levels of succinic acid (Figure 3). The substantial surge of lactic acid in the Raisin group establishes a low-pH environment, which is the primary driver for acid-induced hydrolysis and chemical esterification within the bread. These diverging acid profiles represent a fundamental shift in the chemical environment, where the acidic conditions of the raisin group actively catalyze the transformation of the volatile profile.

Carbohydrate metabolism displayed a similar contrast. The yeast control displayed metabolic depletion, with consistently low sugar levels (Day 0–3) suggesting insufficient enzymatic activity or limiting retrogradation effects. Conversely, the Raisin-Sourdough group demonstrated a significant net accumulation of sugars (Figure 3), implying that acid hydrolysis driven by organic acids continued to degrade the starch matrix post-baking faster than the sugars were consumed. By enriching hydroxyl (-OH) content and acting as a substrate for non-enzymatic browning, these retained sugars sustain the aromatic complexity that is depleted in the control group. This metabolic surplus in the raisin group ensures a persistent supply of reactive molecules that can participate in aroma evolution during shelf life.

Overall, these metabolic shifts confirm that the raisin substrate generates a distinct acidic environment enriched with flavor precursors and residual sugars. This abundant reservoir of non-volatile metabolites likely contributes to the sustained complexity of the aroma profile observed during the shelf life.

Alongside these metabolic characterizations, the potential dominant microorganisms from existing literature were categorized into lactic acid bacteria (LAB)—such as *L. paracasei*, *L. brevis*, and *W. cibaria*—and yeasts (e.g., *C. krusei*, *H. uvarum*) (Table 5). Primary metabolites analysis revealed that the raisin syrup sourdough group was characterized by a distinct accumulation of organic acids and free amino acids, contrasting with the depletion observed in the yeast control. This metabolic footprint is critical, as the combination of high lactic acid production and extensive amino acid release suggests the fermentation is driven primarily by the LAB identified in the reference table rather than the yeast species [20].

Table 5. Dominant Microorganisms Identified in Raisin and Grape Sourdoughs.

Strain Name	Species	References
Lactobacillus paracasei	LAB	[17,21]
Lactobacillus brevis	LAB	[1,22]
Pediococcus pentosaceus	LAB	[22,23]
Weissella cibaria	LAB	[22]
Lactobacillus plantarum	LAB	[1]
Lactobacillus sanfranciscensis	LAB	[4,24]
Candida krusei	Yeast	[25]
Torulaspora delbrueckii	Yeast	[25]
Hanseniaspora uvarum	Yeast	[25]
Hanseniaspora vineae	Yeast	[26]

3.4. Functional Group Analysis

Based on the heatmap and PCA results that verified sample divergence across shelf life, the dynamic VOC patterns were further summarized at the functional-group level to describe class-wise temporal shifts. The most significant early transformation involved alcohols, mirroring the kinetic divergence in the HCA dendrogram. While the Raisin group's alcohol content plummeted by 30% from Day 0 to Day 1 and subsequently stabilized at 22.71% by Day 3, the Yeast control demonstrated a distinct temporal lag. Alcohols decreased more conservatively by 7% on Day 1 and reached a 16% reduction by Day 3 in the yeast group, consistent with the delayed aroma profile evolution shown in Figure 4A.

This rapid shift in the raisin group is likely driven by the specific organic acid profile produced during fermentation. The substantial surge of lactic acid in the raisin group establishes a low-pH environment, which serves as the primary driver for chemical esterification. In this acidic environment, acetic acid likely reacts with alcohols to form volatile acetate esters, thereby sequestering alcohols into a stable fruity equilibrium [27].

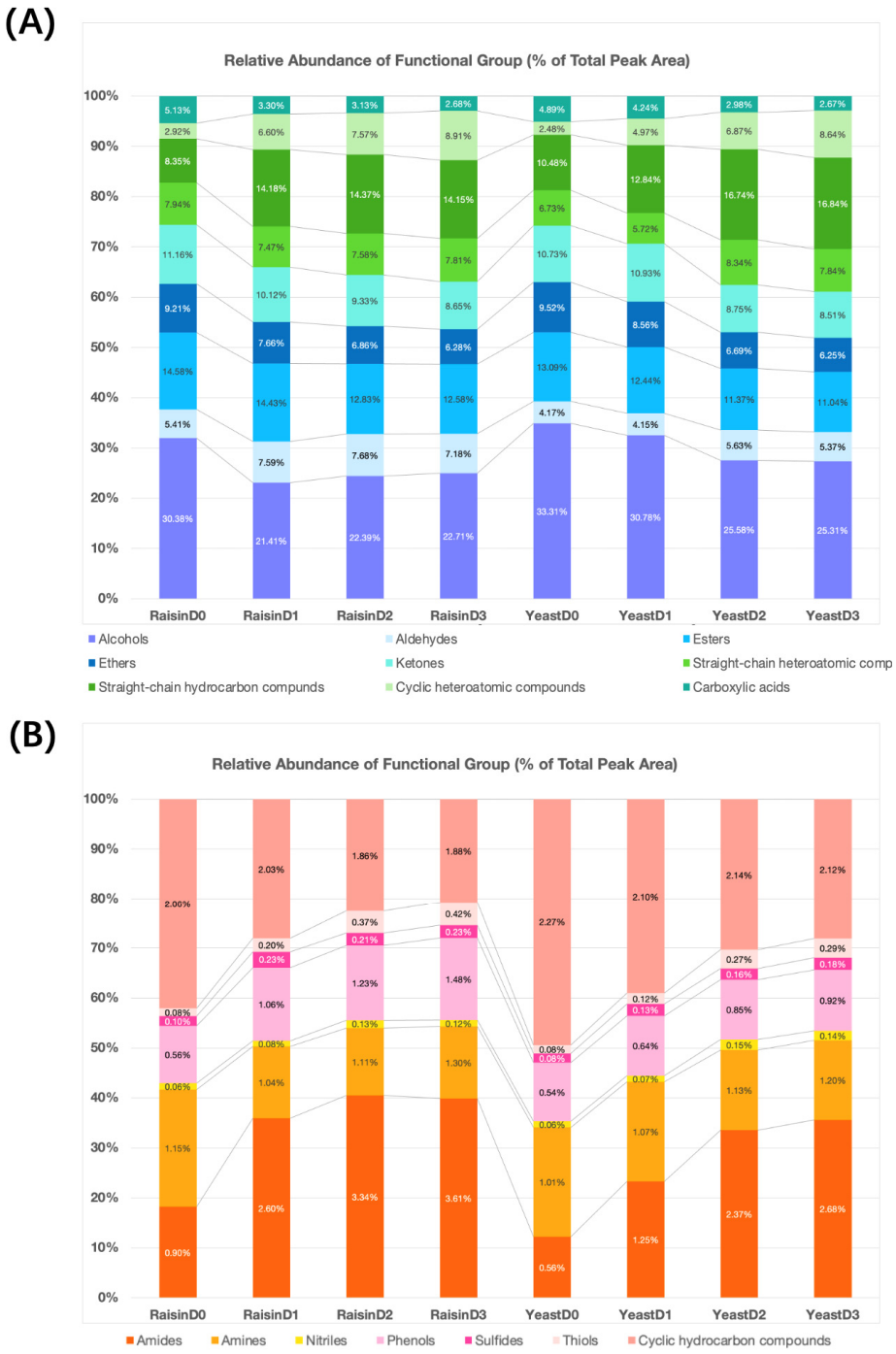

Figure 4. Relative abundance of volatile functional groups in Raisin and Yeast bread during shelf life storage. (**A**) Distribution of major functional groups (high relative abundance), including alcohols, aldehydes, and esters. (**B**) Distribution of minor functional groups (low relative abundance), including amides, amines, and phenols. The stacked bars represent the percentage of the total peak area for each functional group across four time points (D0–D3).

This chemical transition is reflected in the ester behavior, which remained more pronounced in the raisin sourdough than in the yeast control by Day 3 (12% higher). Importantly, the key distinction was not only the end-point difference but also the time-course stability. Ester contribution declined in the yeast control across shelf life, whereas the raisin group stayed largely unchanged. This sustained ester profile suggests a more stable late-stage maturation pattern in the raisin sourdough, which likely underlies the clearer separation of the two groups observed in the HCA and PCA results (Figure 4A).

A complementary shift was observed in aldehydes and alcohols. Aldehydes increased as alcohols declined, suggesting progressive oxidative conversion during early storage. In the raisin sourdough, aldehydes rose rapidly by Day 1 and then remained relatively stable through Day 3, whereas the yeast control stayed at a lower level (Figure 4A). This pattern is consistent with conversion of alcohol precursors to branched-chain aldehydes under the post-baking chemical environment established by sourdough fermentation [3], potentially contributing to aroma retention during storage. These conversions suggest that raisin sourdough can better preserve aroma during storage against oxidation, potentially mitigating staling and supporting shelf life stability without synthetic flavor additives.

Primary metabolite analysis further indicated that sourdough fermentation enriched the pool of total free amino acids. Although microbial metabolism ceases after baking, retained branched-chain amino acids can serve as precursor reservoirs for non-enzymatic Strecker degradation during storage, generating malty and nutty Strecker aldehydes. This mechanism helps explain the higher levels of these aldehyde markers in sourdough samples and suggests that the sourdough matrix functions as a precursor reservoir, partially offsetting volatile loss during staling and thereby supporting aroma retention during shelf life as an efficient stabilizer [28,29].

Importantly, aldehyde enrichment should be distinguished from rancidity-driven lipid oxidation. Functional-group patterns suggest that the aldehyde increase in the Raisin sourdough is not dominated by undesirable lipid oxidation, as the yeast control showed a higher contribution of straight-chain hydrocarbons at Day 3, which is commonly associated with lipid oxidation (Figure 4A). The reduced formation of rancidity products in the raisin group may be linked to stronger acidification (higher lactic and citric acids), which can suppress lipase activity and subsequent formation of straight-chain oxidation products [1,4]. Therefore, elevated aldehydes in the raisin samples more plausibly reflect fermentation-associated transformations rather than rancidity, aligning with the group separation observed in HCA and PCA.

Cyclic heteroatomic compounds increased sharply during the first 24 h in the raisin sourdough, indicating an accelerated early-stage rise in heterocycle-related volatiles compared with the yeast control (Figure 4B). This pattern aligns with the group separation observed in HCA/PCA, suggesting that these compounds contribute to the divergence between treatments. Potential explanation is that raisin fermentation enriches Maillard precursors (sugars and hydrophobic amino acids), as supported by the primary metabolite analysis, promoting greater heterocycle formation during baking. The subsequent increase during storage may reflect gradual release from the crumb matrix rather than de novo post-baking synthesis [17]. It suggests that most raisin sourdough aroma is established during baking, while the bread matrix helps retain these profiles and supports fresh-like aroma early in shelf life.

Similarly, amides and phenols showed a clearer separation between the two groups toward the end of shelf life, reinforcing the divergent maturation trajectories suggested by HCA/PCA (Figure 4B). Simultaneously, phenols were drastically 60% more abundant in the raisin samples compared to the control. These elevated concentrations suggest a more intensive maturation process and are likely driven by acid accumulation, which activates proteolytic enzymes and solubilizes bound phenolic acids effectively trapped within the starch–protein network [4], directly increasing the concentration of savory flavor compounds and complex aroma markers.

These findings demonstrate that raisin syrup sourdough offers superior aromatic quality compared to yeast control. Although both groups maintained a stable count of ~760–765 volatile compounds, the underlying drivers differed significantly. The yeast control accumulated oxidative byproducts, whereas the raisin sourdough preserved and

generated fresh aroma compounds. This confirms that the sourdough process effectively replaces oxidative decay with aromatic integrity.

3.5. Volcano Plot Analysis

To comprehensively map the metabolic shifts driving the observed separation, we performed a systematic differential analysis using volcano plots (Figure 5). The complete set of pairwise comparison volcano plots are provided in Supplementary Material Figures S1–S4.

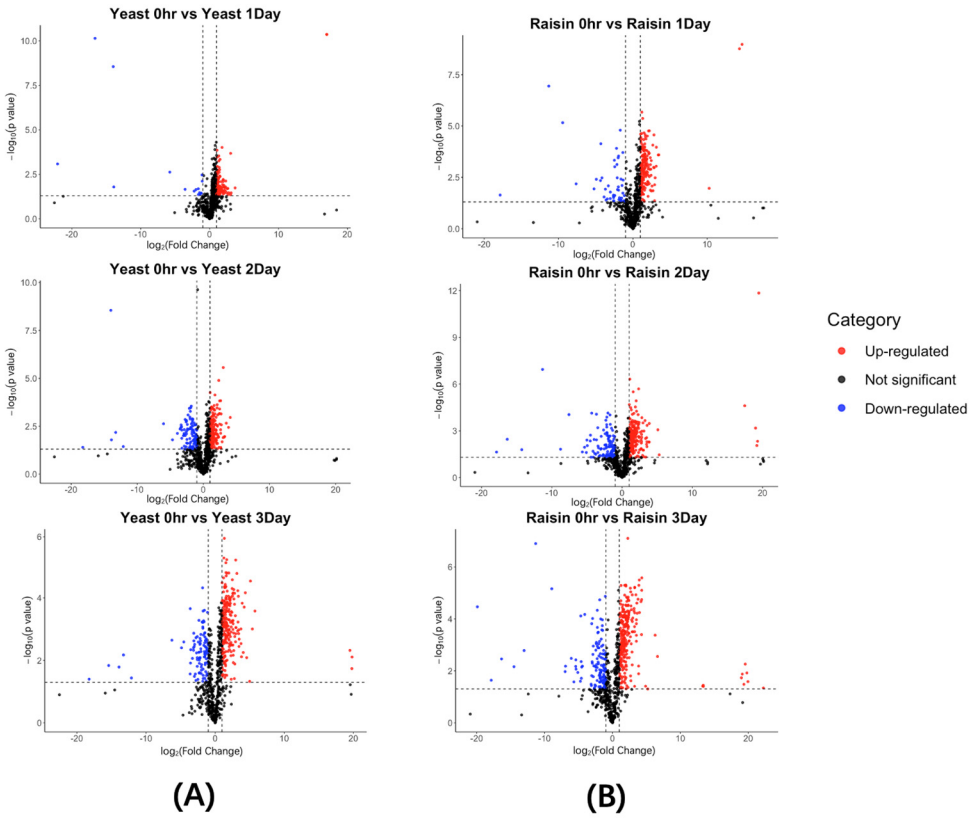

Figure 5. Volcano plot analysis of volatile metabolites across fermentation stages. (**A**) Pairwise comparisons of Yeast (Control) relative to baseline: D0 vs. D1 (top), D0 vs. D2 (middle), and D0 vs. D3 (bottom). (**B**) Pairwise comparisons of Raisin sourdough relative to baseline: D0 vs. D1 (top), D0 vs. D2 (middle), and D0 vs. D3 (bottom). Each point represents a single volatile feature. Red dots denote significantly up-regulated compounds ($\log_2$FC ≥ 1, $p < 0.05$); Blue dots denote significantly down-regulated compounds ($\log_2$FC ≤ -1, $p < 0.05$); Black dots indicate no statistical significance.

Among these comparisons, the longitudinal analysis revealed distinct aroma evolution between the two groups. Within the first 24 h, the raisin water sourdough generated nearly twice as many differential metabolites as the yeast control (182 vs. 99). This advantage persisted through shelf life, with a higher total at Day 3 (275 vs. 230), supporting a stronger flavor-forming capacity of the sourdough process. Collectively, the data indicate that sourdough establishes a richer aroma baseline early on, which is technologically relevant for achieving greater flavor complexity than commercial yeast in the initial stages.

These quantitative trends are supported by marker compounds that align with prior studies, most of which used HS-SPME-GC-MS or related headspace approaches. The sourdough samples showed higher levels of volatiles frequently reported for sourdough aroma, including 2-heptanone (fruity/blue-cheese notes), 2-furanmethanol (caramel/burnt sugar), 2,4-decadienal (fatty/fried), and 1-penten-3-ol (grassy/fresh), consistent with [17,19,30]. In contrast, the yeast control was characterized by 1-propanol, acetoin, and hexanoic acid, in agreement with profiles reported by earlier reports [24]. Collectively, these comparisons

indicate that yeast leavening follows a more conventional alcohol and buttery trajectory, whereas raisin sourdough exhibits a broader volatile profile with stronger fruity, toasted, and green notes.

3.6. Identification and Temporal Profiling of Key Aroma Markers

Following the relevance hierarchy defined in Section 2.5, the prioritized key markers were tracked using dumbbell plots with sparkline-normalized trends to visualize their Day 0–Day 3 evolution.

At the end of shelf life (Day 3), the dumbbell spans in Figure 6 reveal a sharp stratification between the sourdough and control groups. This disparity is driven by the interplay between post-baking flavor baseline at Day 0 (Figure 7) and divergent kinetic rates during storage.

For the markers in Panel A of raisin-dominated profile, the dumbbell plot highlights a profound magnitude of difference, with the raisin sourdough (Red) maintaining significantly higher $\log_{10}$ peak areas than the yeast control (Blue) (Figure 6). This dominance is primarily highlighted by a massive initial flavor load established immediately post-baking (Day 0) (Figure 7). This suggests that raisin sourdough drives aroma synthesis more efficiently than commercial yeast, building a higher initial aroma load during proofing that enriches the bread before storage, supporting longer retention of desirable arom during shelf life as a stronger bio-flavoring system.

Specifically, benzenepropanol, which showed >80% relative abundance in the raisin group at Day 0 (Figure 7) contributes to fruity, floral, and balsamic aroma to the crumb and is likely a product of the Ehrlich pathway, where microbes metabolize phenylalanine during the extended fermentation period [3]. Similarly, octanoate <isopentyl->, also known as isopentyl octanoate, a marker solely dominant in the sourdough, is associated with a distinct fruity and banana-like flavor typical of non-conventional yeast fermentation [31]. Its presence indicates that the sourdough process incorporates unique esterification pathways that are absent in commercial yeast fermentation. Furthermore, 9-Decenoic acid, ethyl ester was also identified as another key contributor, providing a sophisticated aromatic layer characterized by waxy, fruity, and milky notes [31]. This compound is an ester-derived product of lipid metabolism that forms under the slow acidification of sourdough. It is largely absent in the yeast control, where rapid fermentation provides insufficient acidification and lacks the microbial synergy required for these reactions [24]. This interpretation aligns with stronger acidification in the raisin group observed in the primary-metabolite data (Figure 3).

Beyond these primary markers, 2-Ethyl-2-butenal was detected. Though not being reported as a typical key aroma in traditional bread, this unsaturated aldehyde generally contributes to green, grassy, or pungent notes in sourdough [31]. Notably, our analysis also identified 2-Propanamine, N, 2-dimethyl-. Although not reported in standard bread flavor databases, this amine is a marker of amino acid decarboxylation during sourdough fermentation [32]. Its presence is consistent with stronger proteolysis drive by acidification in the raisin group, supported by primary metabolite profiles (Figure 3), and may contribute cheesy or pungent notes as a natural flavoring strategy [4]. The detection of such trace, undocumented compounds highlighted the superior resolving power and innovation of the 2DGC method employed in this study, enabling the characterization of novel flavor contributors that traditional methods might miss.

Beyond this initial advantage, the kinetic data reveals a superior stability mechanism where these compounds exhibited a flat or shallow trajectory in the raisin group. Such trends indicate that the raisin sourdough not only produced these favorable aromas faster

during fermentation but also stabilized them against volatilization to preserve the fruity and floral profile throughout the shelf life.

Conversely, Panel B reflects the yeast-control signature, characterized by isobutanol, acetoin, 2,3-pentanedione, and related small alcohols and ketones (Figure 6). This pattern reflects a largely *S. cerevisiae* driven fermentation, retaining common yeast metabolites and showing more oxidation derived products [17]. In contrast to Panel A, limited acidification and the absence of mixed microbiota likely restrict conversion into more complex secondary compounds. Regarding the metabolic baseline (Figure 7), the yeast control retained 3-fold higher levels of ketones. Isobutanol is a characteristic alcohol via the Ehrlich pathway during standard yeast fermentation and is known to contribute fruity, alcoholic, or malty aromas [28]. Similarly, 2,3-Pentanedione was prevalent in the control group where this metabolite, typically produced by Saccharomyces cerevisiae or Maillard reactions, imparts creamy, oily, or cheesy notes to the crumb [33]. The persistence of these compounds highlights that the yeast control followed a basic metabolic trajectory by retaining simple fermentation byproducts which were otherwise suppressed or chemically converted in the sourdough environment.

However, the clearest kinetic divergence is seen in oxidation-related off-flavor markers. 9,17-octadecadienal (Z)-, an unsaturated aldehyde widely used as a lipid-oxidation biomarker linked to off-flavor development, remained low and essentially unchanged in the raisin sourdough from Day 0 to Day 3, whereas it increased steadily in the yeast control over the same period. This pattern suggests stronger oxidative protection in sourdough, potentially driven by raisin-derived phenolics and gradual acidification that may suppress lipoxygenase and slow lipid oxidation [34]. Consistently, oxidation-related products accumulated more in the yeast control over shelf life, whereas the sourdough samples showed a reduced increase in these markers, without the use of synthetic antioxidants [4].

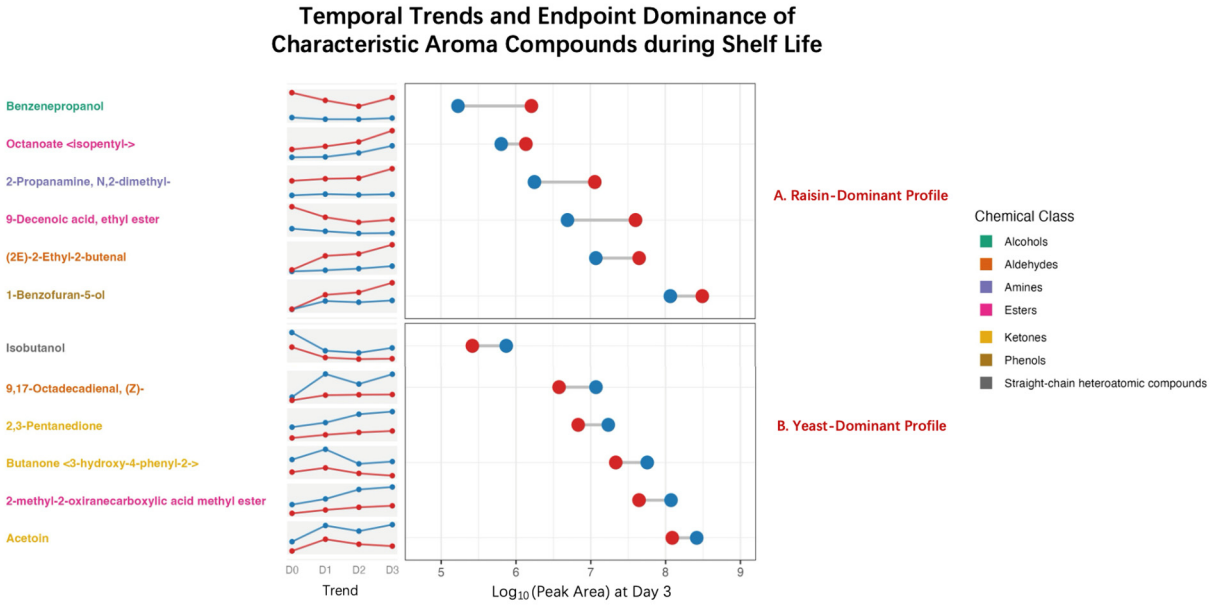

Figure 6. Temporal trends and endpoint dominance of characteristic aroma compounds during shelf life. The figure categorizes key volatile markers into two profiles at Day 3: (**A**) Raisin-Dominant Profile, comprising markers where the raisin sourdough (Red) maintained higher abundance than the yeast control (Blue) at the end of shelf life; and (**B**) Yeast-Dominant Profile, comprising markers where the yeast control exhibited predominant intensity at Day 3. The left side of each panel traces the kinetic trajectory from D0 to D3. The right side visualizes the endpoint disparity using log 10 transformed peak areas, where the length of the connecting line signifies the magnitude of the difference between the two groups—a wider span indicates a more pronounced divergence in flavor intensity.

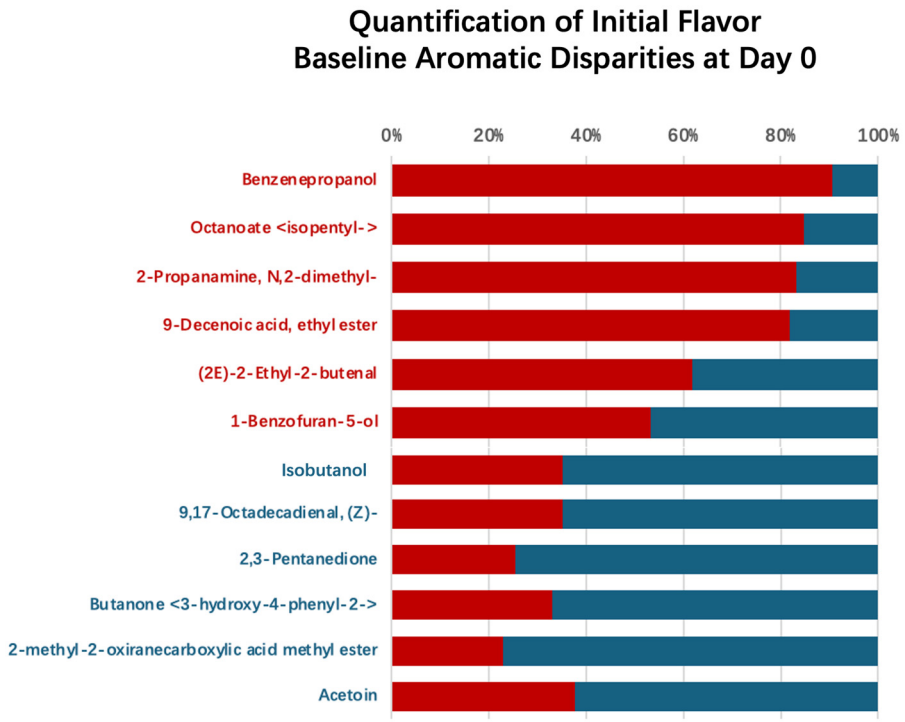

Figure 7. Quantification of initial flavor capital showing baseline aromatic disparities at Day 0. The chart illustrates the relative abundance of characteristic aroma compounds immediately after baking (Day 0). Data represents the percentage contribution of Raisin Sourdough (Red) versus Yeast Control (Blue) to the total raw peak area intensity for each marker.

4. Conclusions

Utilizing comprehensive GC × GC-MS, this study resolved over 760 volatiles in Japanese raisin syrup sourdough, uncovering contributors typically masked by co-elution. Results revealed a kinetic divergence where commercial yeast exhibited a 24 h metabolic lag, while the raisin syrup starter achieved rapid activation and complex flavor synthesis by Day 1. Specifically, the raisin sourdough established a superior and stable aromatic profile during storage by rapidly synthesizing and stabilizing key fruity, green and cheesy markers, represented by benzenepropanol, isopentyl octanoate, and 9-decenoic acid, ethyl ester. In contrast, the yeast control was dominated by standard malty, buttery and alcoholic fermentation markers (isobutanol, acetoin, and 2,3-pentanedione) and was kinetically compromised by a faster accumulation of lipid-oxidation products, as indicated by 9,17-octadecadienal.

However, chemical profiles do not necessarily translate into perceived flavor. Due to practical constraints, odor activity values (OAVs) were not quantified, and consequent sensory relevance of individual odorants and the perceptibility of the observed compositional shifts cannot be fully established. Accordingly, future studies should integrate OAV-based prioritization with sensory evaluation to validate these effects. In addition, limited microbial characterization hinders the linkage between microbial activity and flavor formation, highlighting the need for targeted strain identification to clarify flavor-development and activation mechanisms. Overall, this study supports more predictable artisanal practice and provides a blueprint for scaling raisin syrup sourdough into real-world manufacturing and supply chain settings, while demonstrating the analytical capability of comprehensive 2DGC-TOFMS for high-resolution volatile profiling in complex fermented food matrices.

Supplementary Materials: The following supporting information can be downloaded at: https://www.mdpi.com/article/10.3390/foods15040717/s1, Figure S1:Volcano plot analysis of Pairwise comparisons of Yeast sourdough vs. Raisin sourdough D0; Figure S2: Volcano plot analysis of Pairwise comparisons of Yeast sourdough vs. Raisin sourdough D1; Figure S3: Volcano plot analysis of Pairwise comparisons of Yeast sourdough vs. Raisin sourdough D2; Figure S4: Volcano plot analysis of Pairwise comparisons of Yeast sourdough vs. Raisin sourdough D3.

Author Contributions: J.Z.: Data curation, Formal analysis, Methodology, Software, Visualization, Investigation, Writing—original draft; T.M.: Funding acquisition, Methodology, Project administration, Resources, Validation, Writing—review and editing, Software; S.N.: Data curation, Methodology, Investigation; K.S.: Methodology, Resources, Supervision; Y.I.: Resources, Supervision; T.T.: Software, Methodology, Data curation; S.I.: Data curation, Methodology, Investigation; K.H.: Resources, Supervision; T.A.: Project administration, Resources, Supervision. All authors have read and agreed to the published version of the manuscript.

Funding: The project was funded by the Iijima Tojuro Memorial Foundation for Food Science and Technology, Joint Research Grant, Registration Number 3 (FY2021).

Data Availability Statement: The original contributions presented in the study are included in the article/Supplementary Materials, further inquiries can be directed to the corresponding author.

Acknowledgments: The authors would like to express their sincere gratitude to Koji Takeya from TSUMUGI Bakery and Cafe for his expert guidance and technical support in bread production. The authors used generative AI Gemini 3 Flash to improve the language and readability of this manuscript. Following this process, the authors reviewed and edited the content and take full responsibility for the final version of the work.

Conflicts of Interest: The authors declare no conflicts of interest.

Abbreviations

The following abbreviations are used in this manuscript:

LAB	Lactic acid bacteria
GC × GC-TOFMS	Gas chromatography–mass spectrometry
VOCs	Volatile organic compounds

References

1. Fernández-Peláez, J.; Paesani, C.; Gómez, M. Sourdough Technology as a Tool for the Development of Healthier Grain-Based Products: An Update. *Agronomy* **2020**, *10*, 1962. [CrossRef]
2. Torreggiani, A.; Demarinis, C.; Pinto, D.; Papale, A.; Difonzo, G.; Caponio, F.; Pontonio, E.; Verni, M.; Rizzello, C.G. Up-Cycling Grape Pomace through Sourdough Fermentation: Characterization of Phenolic Compounds, Antioxidant Activity, and Anti-Inflammatory Potential. *Antioxidants* **2023**, *12*, 1521. [CrossRef]
3. Lutter, L.; Jõudu, I.; Andreson, H. Volatile Organic Compounds and Their Generation in Sourdough. *Agron. Res.* **2023**, *21*, 504–536. [CrossRef]
4. Hwang, J.-Y.; Shyu, Y.-S. Influence of Raisin Starter Syrup Concentrations on the Properties of Sourdough and Sourdough Bread. *J. Mar. Sci. Technol.* **2015**, *23*, 6. [CrossRef]
5. Górecki, T.; Harynuk, J.; Panić, O. The evolution of comprehensive two-dimensional gas chromatography (GC × GC). *J. Sep. Sci.* **2004**, *27*, 359–379. [CrossRef]
6. Dias, R.P.; Johnson, T.A.; Ferrão, L.F.V.; Munoz, P.R.; De La Mata, A.P.; Harynuk, J.J. Improved sample storage, preparation and extraction of blueberry aroma volatile organic compounds for gas chromatography. *J. Chromatogr. Open* **2023**, *3*, 100075. [CrossRef]
7. Nam, S.; De La Mata, A.; Harynuk, J. Automated Screening and Filtering Scripts for GC × GC-TOFMS Metabolomics Data. *Separations* **2021**, *8*, 84. [CrossRef]
8. Sorochan Armstrong, M.D.; Arredondo Campos, O.R.; Bannon, C.C.; De La Mata, A.P.; Case, R.J.; Harynuk, J.J. Global metabolome analysis of *Dunaliella tertiolecta*, *Phaeobacter italicus* R11 Co-cultures using thermal desorption—Comprehensive two-dimensional gas chromatography—Time-of-flight mass spectrometry (TD-GC × GC-TOFMS). *Phytochemistry* **2022**, *195*, 113052. [CrossRef] [PubMed]

9. Editorial Committee of "Hakkotane to Pan". *Hakkotane to Pan: Kagaku Kara Ōyō Made [Fermented Starters and Bread: From Science to Application]*; Asahiya Publishing: Tokyo, Japan, 2023.
10. Arora, K.; Rizzello, C.G.; Gobbetti, M. How to Prepare, Propagate, and Use the Sourdough. In *Basic Methods and Protocols on Sourdough*; Gobbetti, M., Rizzello, C.G., Eds.; Methods and Protocols in Food Science; Humana: New York, NY, USA, 2024. [CrossRef]
11. Don, C. Dough rheology and the Farinograph: The mechanism underlying dough development. In *The Farinograph Handbook*; Woodhead Publishing: Cambridge, UK, 2022; pp. 43–70.
12. Tsunokawa, J.; Ochiai, N.; Sasamoto, K.; Hoffmann, A. 2-Step Multi-Volatile Method (2-Step MVM) for Characterization of Aroma Compounds in Bread. In *Gerstel Application Note*; Gerstel: Mülheim an der Ruhr, Germany, 2016.
13. GL Sciences. (n.d.). Available online: https://www.glsciences.com/ (accessed on 9 November 2025).
14. InertCap WAX-HT | Products | GL Sciences. Glsciences.com. 2025. Available online: https://www.glsciences.com/product/gc_capillary_columns/inertcap/00142.html?utm_source (accessed on 20 June 2025).
15. InertCap 5MS/NP. GL Science. 2021. Available online: https://www.glsciences.eu/gc-columns/InertCap_5MS-NP_Technical_Information.pdf?utm_source (accessed on 20 June 2025).
16. Pongsuwan, W.; Fukusaki, E.; Bamba, T.; Yonetani, T.; Yamahara, T.; Kobayashi, A. Prediction of Japanese Green Tea Ranking by Gas Chromatography/Mass Spectrometry-Based Hydrophilic Metabolite Fingerprinting. *J. Agric. Food Chem.* **2007**, *55*, 231–236. [CrossRef]
17. Chiavaro, E.; Vittadini, E.; Musci, M.; Bianchi, F.; Curti, E. Shelf-Life Stability of Artisanally and Industrially Produced Durum Wheat Sourdough Bread ("Altamura Bread"). *LWT-Food Sci. Technol.* **2008**, *41*, 58–70. [CrossRef]
18. Bianchi, A.; Venturi, F.; Palermo, C.; Taglieri, I.; Angelini, L.G.; Tavarini, S.; Sanmartin, C. Primary and Secondary Shelf-Life of Bread as a Function of Formulation and MAP Conditions: Focus on Physical-Chemical and Sensory Markers. *Food Packag. Shelf Life* **2024**, *41*, 101241. [CrossRef]
19. Lafuente, C.; Nazareth, T.D.M.; Dopazo, V.; Meca, G.; Luz, C. Enhancing Bread Quality and Extending Shelf Life Using Dried Sourdough. *LWT* **2024**, *203*, 116379. [CrossRef]
20. Kaseleht, K.; Paalme, T.; Mihhalevski, A.; Sarand, I. Analysis of Volatile Compounds Produced by Different Species of Lactobacilli in Rye Sourdough Using Multiple Headspace Extraction. *Int. J. Food Sci. Technol.* **2011**, *46*, 1940–1946. [CrossRef]
21. Aplevicz, K.S.; Mazo, J.Z.; Ilha, E.C.; Dinon, A.Z.; Sant'anna, E.S. Isolation and Characterization of Lactic Acid Bacteria and Yeasts from the Brazilian Grape Sourdough. *Braz. J. Pharm. Sci.* **2014**, *50*, 321–327. [CrossRef]
22. Gordún, E.; Del Valle, L.J.; Ginovart, M.; Carbó, R. Comparison of the Microbial Dynamics and Biochemistry of Laboratory Sourdoughs Prepared with Grape, Apple and Yogurt. *Food Sci. Technol. Int.* **2015**, *21*, 428–439. [CrossRef] [PubMed]
23. Maino, M.-L.; Marc, A.R.; Mureșan, C.C. Functional Plant Substrates in Sourdough Fermentation: Hops, Kombucha, and Grape Pomace. *Hop Med. Plants* **2024**, *32*, 35–55. [CrossRef]
24. Warburton, A.; Silcock, P.; Eyres, G.T. Impact of Sourdough Culture on the Volatile Compounds in Wholemeal Sourdough Bread. *Food Res. Int.* **2022**, *161*, 111885. [CrossRef] [PubMed]
25. Liu, Y.-C.; Wu, P.-S.; Teng, S.-H.; Wu, M.-J. Identification of Dominant Microbes and Functional Analysis of Sourdough Starters Made of Dried Longan and Raisin. *Eng. Proc.* **2023**, *55*, 17. [CrossRef]
26. Takaya, M.; Ohwada, T.; Oda, Y. Characterization of the Yeast *Hanseniaspora vineae* Isolated from the Wine Grape "Yamasachi" and Its Use for Bread Making. *Food Sci. Technol. Res.* **2019**, *25*, 835–842. [CrossRef]
27. Xu, D.; Zhang, Y.; Tang, K.; Hu, Y.; Xu, X.; Gänzle, M.G. Effect of Mixed Cultures of Yeast and Lactobacilli on the Quality of Wheat Sourdough Bread. *Front. Microbiol.* **2019**, *10*, 2113. [CrossRef]
28. Plessas, S.; Bekatorou, A.; Gallanagh, J.; Nigam, P.; Koutinas, A.A.; Psarianos, C. Evolution of Aroma Volatiles during Storage of Sourdough Breads Made by Mixed Cultures of *Kluyveromyces marxianus* and *Lactobacillus delbrueckii* ssp. *Bulgaricus* or *Lactobacillus helveticus*. *Food Chem.* **2008**, *107*, 883–889. [CrossRef]
29. Birch, A.N.; Petersen, M.A.; Hansen, Å.S. The Aroma Profile of Wheat Bread Crumb Influenced by Yeast Concentration and Fermentation Temperature. *LWT-Food Sci. Technol.* **2013**, *50*, 480–488. [CrossRef]
30. Pradal, I.; Weckx, S.; De Vuyst, L. 'The Production of Esters by Specific Sourdough Lactic Acid Bacteria Species Is Limited by the Precursor Concentrations' edited by D. Ercolini. *Appl. Environ. Microbiol.* **2025**, *91*, e02216-24. [CrossRef]
31. Narisawa, T.; Ebara, M.; Harada, M.; Umino, M.; Kaneko, M.; Nakajima, H. The effects of high-ash stream flour on the sourdough properties and the taste and flavor of bread. *Nippon Shokuhin Kagaku Kogaku Kaishi* **2024**, *71*, 231–249. [CrossRef]
32. Kondybayev, A.; Zhakupbekova, A.; Amutova, F.; Omarova, A.; Nurseitova, M.; Akhmetsadykova, S.; Akhmetsadykov, N.; Konuspayeva, G.; Faye, B. Volatile Organic Compounds Profiles in Milk Fermented by Lactic Bacteria. *Int. J. Biol. Chem.* **2018**, *11*, 57–67. [CrossRef]

33. Maeda, T.; Kikuma, S.; Araki, T.; Ikeda, G.; Takeya, K.; Sagara, Y. The Effects of Mixing Stage and Fermentation Time on the Quantity of Flavor Compounds and Sensory Intensity of Flavor in White Bread. *Food Sci. Technol. Res.* **2009**, *15*, 117–126. [CrossRef]
34. Quílez, J.; Ruiz, J.A.; Romero, M.P. Relationships Between Sensory Flavor Evaluation and Volatile and Nonvolatile Compounds in Commercial Wheat Bread Type Baguette. *J. Food Sci.* **2006**, *71*, 423–427. [CrossRef]

Disclaimer/Publisher's Note: The statements, opinions and data contained in all publications are solely those of the individual author(s) and contributor(s) and not of MDPI and/or the editor(s). MDPI and/or the editor(s) disclaim responsibility for any injury to people or property resulting from any ideas, methods, instructions or products referred to in the content.